

1 **PRMT5 regulates ovarian follicle development by facilitating *Wt1***
2 **translation**

3 Min Chen^{1,2,#,&}, Fangfang Dong^{1,2,3#}, Min Chen^{4,&}, Zhiming Shen^{1,2,3}, Haowei Wu^{1,2,3}, Changhuo
4 Cen^{1,2,3}, Xiuhong Cui^{1,2}, Shilai Bao⁵, Fei Gao^{1,2,3,*}

5
6 ¹State Key Laboratory of Stem Cell and Reproductive Biology, Institute of Zoology,
7 Chinese Academy of Sciences, Beijing, 100101, P. R. China

8 ²Institute for Stem Cell and Regeneration, Chinese Academy of Sciences, Beijing
9 100101, P. R. China

10 ³University of Chinese Academy of Sciences, Beijing, 100049, P. R. China

11 ⁴Guangdong and Shenzhen Key Laboratory of Male Reproductive Medicine and
12 Genetics, Institute of Urology, Peking University Shenzhen Hospital, Shenzhen
13 Peking University-Hong Kong University of Science and Technology Medical Center,
14 Shenzhen, Guangdong 518036, P. R. China

15 ⁵State Key Laboratory of Molecular Developmental Biology, Institute of Genetics and
16 Developmental Biology, Chinese Academy of Sciences, Beijing, 100101, P. R. China

17 #Co-first author

18 *Correspondence to: Fei Gao, gaof@ioz.ac.cn (F.G.)

19 &The same name for different person

20

21 **Running title:** PRMT5 in follicle development

22

23 **Abstract**

24 Protein arginine methyltransferase 5 (*Prmt5*) is the major type II enzyme
25 responsible for symmetric dimethylation of arginine. Here, we found PRMT5 was
26 expressed at high level in ovarian granulosa cells of growing follicles. Inactivation of
27 *Prmt5* in granulosa cells resulted in aberrant follicle development and female
28 infertility. In *Prmt5*-knockout mice, follicle development was arrested with
29 disorganized granulosa cells in which WT1 expression was dramatically reduced and
30 the expression of steroidogenesis-related genes was significantly increased. The
31 premature differentiated granulosa cells were detached from oocytes and follicle
32 structure was disrupted. Mechanism studies revealed that *Wtl* expression was
33 regulated by PRMT5 at the protein level. PRMT5 facilitated IRES-dependent
34 translation of *Wtl* mRNA by methylating HnRNPA1. Moreover, the upregulation of
35 steroidogenic genes in *Prmt5*-deficient granulosa cells was repressed by *Wtl*
36 overexpression. These results demonstrate PRMT5 participates in granulosa cell
37 lineage maintenance by inducing *Wtl* expression. Our study uncovers a new role of
38 post-translational arginine methylation in granulosa cell differentiation and follicle
39 development.

40

41 **Keywords:** ovary; granulosa cells; PRMT5; *Wtl*; IRES

42

43 **Introduction**

44 Follicles are the basic functional units in the ovaries. Each follicle consists of an
45 oocyte, the surrounding granulosa cells and theca cells in the mesenchyme. The
46 interaction between oocytes and somatic cells is crucial for follicle development.
47 Follicle maturation experiences primordial, primary, secondary, and antral follicular
48 stages. Primordial follicles are formed shortly after birth via breakdown of oocyte
49 syncytia. Each primordial follicle is composed of an oocyte surrounded by a single
50 layer of flattened pregranulosa cells that remains in a dormant phase until being
51 recruited into the primary stage under the influence of two main signaling pathways¹.
52 Once activated, flattened granulosa cells become cuboidal, and follicles continue to
53 grow through proliferation of granulosa cells and enlargement of oocytes.
54 Development of high-quality oocytes is important for female reproductive health and
55 fertility¹⁻⁴. Although gonadotropin, follicle-stimulating hormone (FSH) and
56 luteinizing hormone (LH) are important for the growth of antral follicles, the early
57 stages of follicle development are driven by a local oocyte-granulosa cell dialog.
58 Abnormalities in this process may lead to follicle growth arrest or atresia^{2,5}.

59 Granulosa cells are derived from progenitors of the coelomic epithelium that
60 direct sexual differentiation at the embryonic stage and support oocyte development
61 postnatally^{4,6}. Theca-interstitial cell differentiation occurs postnatally along with the
62 formation of secondary follicles. The steroid hormone produced by theca-interstitial
63 cells plays important roles in follicle development and maintenance of secondary
64 sexual characteristics⁴. The Wilms' tumor (WT) suppressor gene *Wt1* is a nuclear

65 transcription factor indispensable for normal development of several tissues. In
66 gonads, *Wtl* is mainly expressed in ovarian granulosa cells and testicular Sertoli cells.
67 During follicle development, *Wtl* is expressed at high levels in granulosa cells of
68 primordial, primary and secondary follicles, but its expression is decreased in antral
69 follicles⁷. Our previous studies demonstrated that *Wtl* is required for the lineage
70 specification and maintenance of Sertoli and granulosa cells^{8,9}. However, the
71 underlying mechanism that regulates the expression of *Wtl* in granulosa cells is
72 unknown.

73 Protein arginine methyltransferase 5 (PRMT5) is a member of the PRMT family
74 that catalyzes the transfer of methyl groups from S-adenosylmethionine to a variety of
75 substrates and is involved in many cellular processes, such as cell growth,
76 differentiation and development¹⁰⁻¹². PRMT5 is the predominant type II
77 methyltransferase that catalyzes the formation of most symmetric dimethylarginines
78 (SDMAs) in the cells and regulates gene expression at the transcriptional and
79 posttranscriptional levels¹⁰. PRMT5 forms a complex with its substrate-binding
80 partner, the WD-repeat protein MEP50 (or WDR77), which greatly enhances the
81 methyltransferase activity of PRMT5 by increasing its affinity for protein substrates¹¹.

82 In gonad development, inactivation of *Prmt5* specifically in primordial germ
83 cells (PGCs) causes massive loss of PGCs¹³⁻¹⁵. PRMT5 promotes PGC survival by
84 regulating RNA splicing¹³ and suppressing transposable elements at the time of global
85 DNA demethylation¹⁴. In this study, we found that PRMT5 is expressed at high level
86 in ovarian granulosa cells of growing follicles and the expression level changes with

87 follicle development, suggesting that PRMT5 in granulosa cells plays a role in follicle
88 development. To test the function of PRMT5 in granulosa cells, we specifically
89 inactivated *Prmt5* in granulosa cells using *Sfl-cre*. We found that *Prmt5^{lox/lox};Sfl-cre*
90 female mice were infertile and that follicles were arrested at the preantral stage. The
91 expression of WT1 was dramatically reduced, and the granulosa cells in secondary
92 follicles began to express steroidogenic genes. Further studies revealed that PRMT5
93 regulates follicle development by facilitating *Wt1* translation.

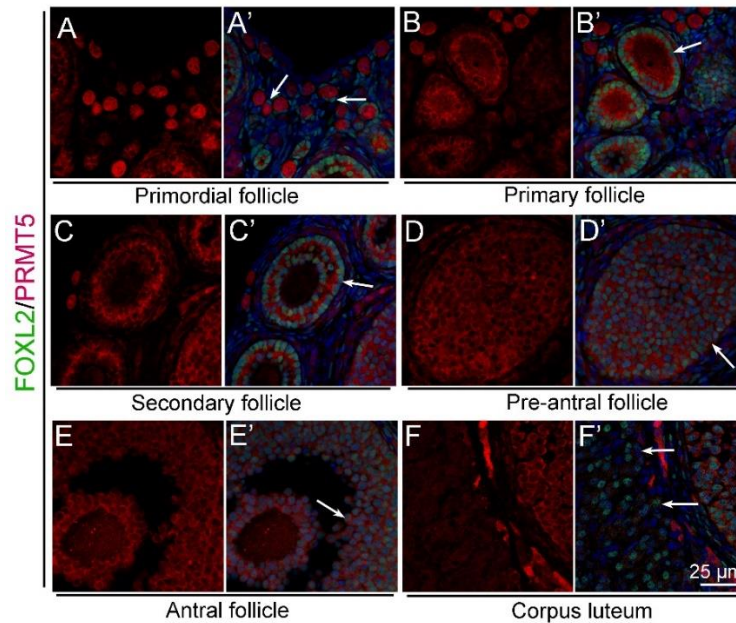
94

95 **Results**

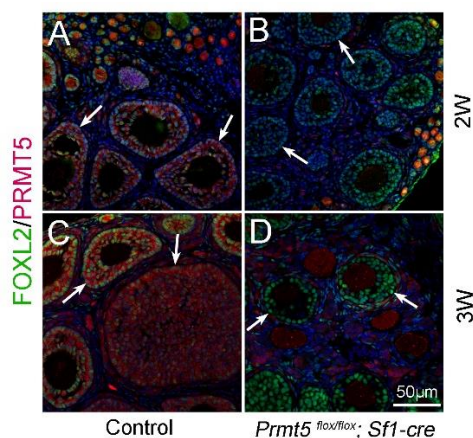
96 *Deletion of Prmt5 in granulosa cells caused aberrant ovary development and female*
97 *infertility.*

98 The expression of PRMT5 in ovarian granulosa cells was examined by
99 immunofluorescence. As shown in Fig. S1, PRMT5 (red) was expressed in oocytes,
100 but no PRMT5 signal was detected in the granulosa cells of primordial follicles (A, A',
101 white arrows). PRMT5 started to be expressed in granulosa cells of primary follicles
102 (B, B', white arrows) and was continuously expressed in granulosa cells of secondary
103 follicles (C, C', white arrows), preantral follicles (D, D', white arrows), and antral
104 follicles (E, E', white arrows), but its expression decreased significantly in the corpus
105 luteum (F, F', white arrows). To test the functions of PRMT5 in granulosa cell
106 development, we specifically deleted *Prmt5* in granulosa cells by crossing *Prmt5^{lox/lox}*
107 mice with *Sfl-cre* transgenic mice. In *Prmt5^{lox/lox};Sfl-cre* female mice, PRMT5
108 expression was completely absent from granulosa cells (Fig. S2, arrows in B, D),

109 whereas the expression of PRMT5 in oocytes and interstitial cells was not affected,
110 suggesting that *Prmt5* was specifically deleted in granulosa cells.



112 **Figure S1. PRMT5 was expressed in granulosa cells of growing follicles.** The expression of
113 PRMT5 was examined by immunofluorescence (red), and granulosa cells were labeled with
114 FOXL2 (green). PRMT5 was not expressed in granulosa cells of primordial follicles (A, A', white
115 arrows). PRMT5 was expressed in granulosa cells of primary follicles (B, B', white arrows),
116 secondary follicles (C, C', white arrows), preantral follicles (D, D', white arrows), and antral
117 follicles (E, E', white arrows). No PRMT5 signal was detected in the corpus luteum (F, F', white
118 arrows). DAPI (blue) was used to stain the nuclei.



120 **Figure S2. *Prmt5* was deleted in granulosa cells of *Prmt5^{flox/flox}; Sf1-cre* mice.** The expression of
121 PRMT5 was examined by immunofluorescence (red), and granulosa cells were labeled with
122 FOXL2 (green). PRMT5 protein was detected in granulosa cells of control ovaries at 2 weeks (A,
123 white arrows) and 3 weeks (C, white arrows) after birth. No PRMT5 signal was detected in
124 granulosa cells of *Prmt5^{flox/flox}; Sf1-cre* ovaries at 2 weeks (B, white arrows) and 3 weeks (D, white
125 arrows). DAPI (blue) was used to stain the nuclei.

126 No obvious developmental abnormalities were observed in adult
127 *Prmt5^{flox/flox};Sfl-cre* mice (Fig. 1A). However, the female mice were infertile with
128 atrophic ovaries (Fig. 1B). The results of immunohistochemistry showed growing
129 follicles at different stages in control ovaries at 2 months of age (Fig. 1C). In contrast,
130 only a small number of follicles and few corpora lutea were observed in
131 *Prmt5^{flox/flox};Sfl-cre* mice (Fig. 1D). We further examined follicle development in
132 *Prmt5^{flox/flox};Sfl-cre* mice at different developmental stages. As shown in Fig. 1, a
133 large number of growing follicles at the primary and secondary stages were observed
134 in *Prmt5^{flox/flox};Sfl-cre* mice (F) at 2 weeks, which was comparable to the situation in
135 control ovaries (E). Most of the follicles were at the preantral and antral follicle stages
136 in control mice at 3 weeks (G), whereas the development of follicles in
137 *Prmt5^{flox/flox};Sfl-cre* mice was arrested, and aberrant granulosa cells were observed
138 (H). The defects in follicle development were more obvious at 4 (J) and 5 weeks (L).
139 The number of granulosa cells around oocytes was dramatically reduced, and follicle
140 structure was disrupted.

141

142

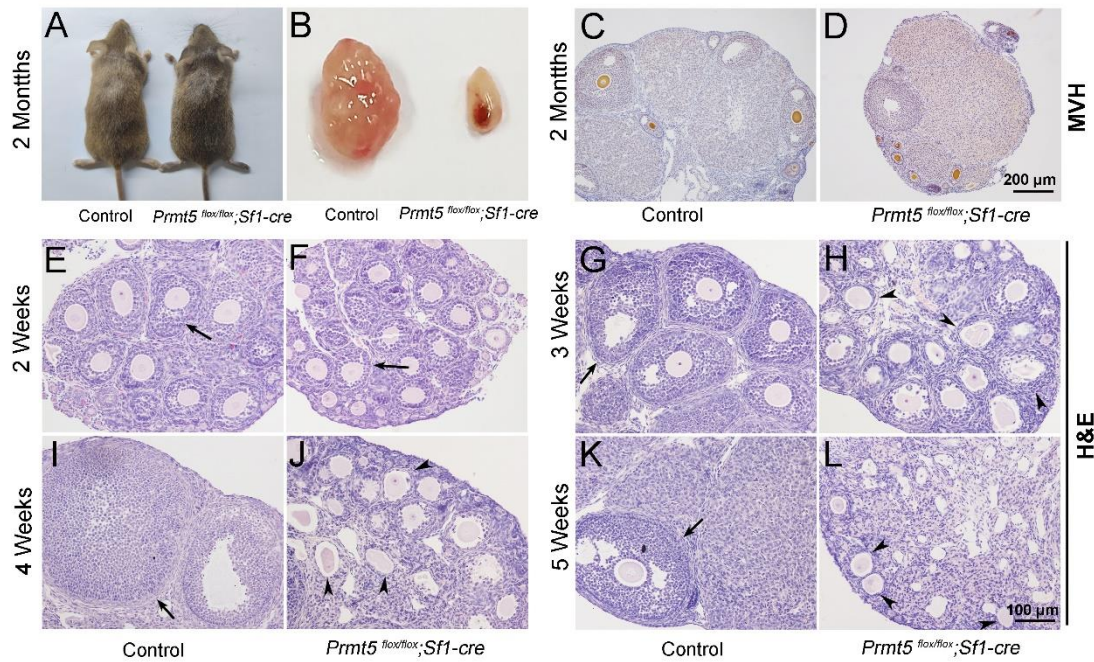
143

144

145

146

147



148

149 **Figure 1. Loss of *Prmt5* in granulosa cells caused aberrant follicle development and female**
150 **infertility.** No developmental abnormalities were observed in *Prmt5^{flox/flox};Sf1-cre* mice (A) at
151 2 months of age, and the ovary size was dramatically reduced (B). Morphology of ovaries from
152 control (C) and *Prmt5^{flox/flox};Sf1-cre* mice (D) at 2 months of age. The morphology of ovarian
153 follicles was grossly normal in *Prmt5^{flox/flox}* mice at 2 weeks (F, black arrows). Defects in follicle
154 development were observed in *Prmt5*-mutant mice at 3 weeks (H, black arrowheads). Aberrant
155 ovarian follicles with disorganized granulosa cells were observed in *Prmt5^{flox/flox};Sf1-cre* mice at 4
156 (J, black arrowheads) and 5 (L, black arrowheads) weeks of age.

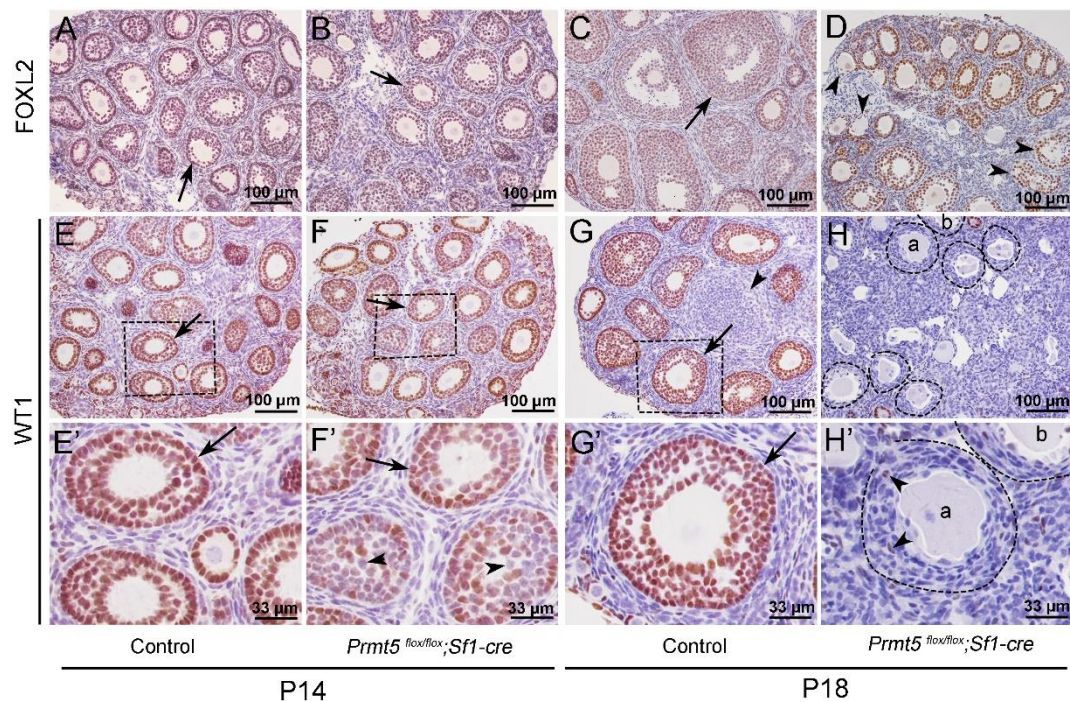
157

158 *The identity of granulosa cells in *Prmt5^{flox/flox};Sf1-cre* mice was changed.*

159 To explore the underlying mechanism that caused the defects in follicle
160 development in *Prmt5^{flox/flox};Sf1-cre* mice, the expression of granulosa cell-specific
161 genes was analyzed by immunohistochemistry. As shown in Fig. 2, FOXL2 protein
162 was expressed in the granulosa cells of both control (A, C) and *Prmt5^{flox/flox};Sf1-cre*
163 mice (B, D) at P14 and P18. WT1 protein was expressed in granulosa cells of primary,
164 secondary and preantral follicles in control mice at P14 and P18 (E, E', G, G', arrows).
165 WT1 was also detected in the follicles of *Prmt5^{flox/flox};Sf1-cre* mice at P14 (F, arrow).
166 However, not all the granulosa cells were WT1-positive; some of them were

167 WT1-negative (F', arrowheads). The WT1 signal was almost completely absent from
168 the majority of granulosa cells in *Prmt5^{fllox/fllox};Sf1-cre* mice at P18 (H, H'); very few
169 granulosa cells were WT1-positive (H', arrowheads). We also found that the
170 granulosa cells in control ovaries were cuboidal and well-organized (G', arrow). In
171 contrast, the granulosa cells in *Prmt5^{fllox/fllox};Sf1-cre* mice were flattened (H', dashed
172 line circle) and were indistinguishable from surrounding stromal cells. The decreased
173 WT1 protein expression in *Prmt5*-deficient granulosa cells was also confirmed by
174 FOXL2/WT1 double staining (Fig. S3).

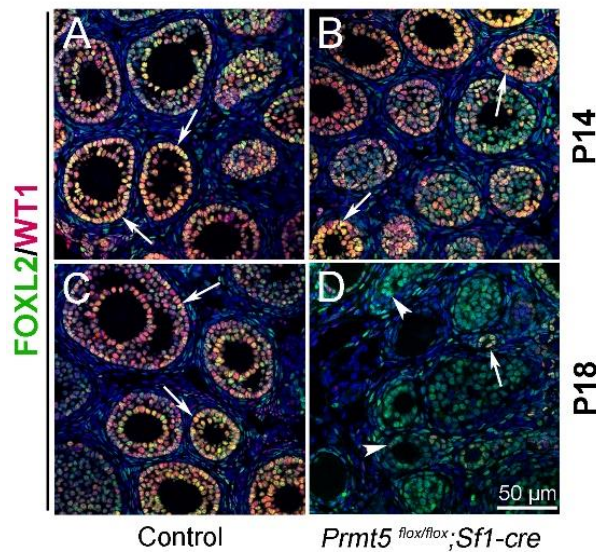
175



176

177 **Figure 2. The expression of WT1 was dramatically reduced in the granulosa cells of**
178 ***Prmt5^{fllox/fllox};Sf1-cre* mice at P18.** The expression of FOXL2 and WT1 in granulosa cells of
179 control and *Prmt5^{fllox/fllox};Sf1-cre* mice was examined by immunohistochemistry. FOXL2 protein
180 was expressed in the granulosa cells of both control (A, C) and *Prmt5^{fllox/fllox};Sf1-cre* mice (B, D) at
181 P14 and P18. WT1 protein was expressed in granulosa cells of primary, secondary and preantral
182 follicles in control mice at P14 and P18 (E, E', G, G', black arrows). WT1 expression was absent
183 from most granulosa cells in *Prmt5^{fllox/fllox};Sf1-cre* mice at P18 (H, H'); only very few granulosa
184 cells were WT1-positive (H', black arrowheads). E'-H' are the magnified views of E-H,
185 respectively.

186



187

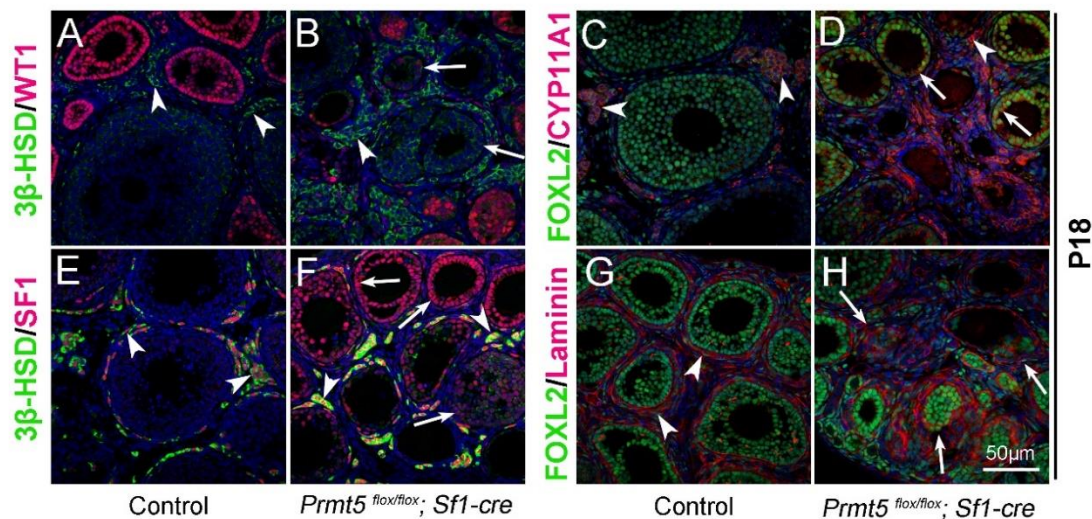
188 **Figure S3. WT1 expression was decreased significantly in *Prmt5^{flox/flox};Sf1-cre* granulosa cells**
189 **at P18.** The expression of FOXL2 (green) and WT1 (red) in ovaries of control and
190 *Prmt5^{flox/flox};Sf1-cre* mice at P14 and P18 was examined by immunofluorescence. WT1 expression
191 was decreased dramatically in *Prmt5^{flox/flox};Sf1-cre* granulosa cells at P18 (D, arrowheads). Few
192 WT1-positive granulosa cells remained (D, arrows). DAPI (blue) was used to stain the nuclei.

193

194 *Wtl* plays a critical role in granulosa cell development, and mutation of *Wtl*
195 leads to pregranulosa cell-to-steroidogenic cell transformation^{8,9}. Therefore, we
196 further examined the expression of steroidogenic genes in *Prmt5*-deficient granulosa
197 cells at P18. As shown in Fig. 3, in control ovaries, 3 β -HSD (3 β -hydroxysteroid
198 dehydrogenase, also known as Hsd3B1) and CYP11A1 (cytochrome P450, family 11,
199 subfamily a, polypeptide 1, also known as P450scc) were expressed in
200 theca-interstitial cells (A, C, arrowheads). In addition to theca-interstitial cells,
201 3 β -HSD (B, green, arrows) and CYP11A1 (D, red, arrows) were also detected in the
202 granulosa cells of *Prmt5^{flox/flox};Sf1-cre* mice. We also examined the expression of SF1
203 (steroidogenic factor 1, also known as NR5A1), which is a key regulator of steroid
204 hormone biosynthesis¹⁶. As expected, SF1 was expressed only in theca-interstitial

205 cells of control ovaries (E, red, arrowheads), whereas a high level of SF1 expression
206 was detected in *Prmt5*-deficient granulosa cells (F, red, arrows), suggesting the
207 identity of granulosa cells was changed. The follicle structure was destroyed as
208 indicated by disorganized Laminin staining (H, arrows). The proliferation and
209 apoptosis of *Prmt5*-deficient granulosa cells were analyzed by BrdU incorporation
210 and TUNEL assays. As shown in Fig. S4, the numbers of TUNEL-positive cells and
211 BrdU-positive granulosa cells were not changed in *Prmt5^{fllox/fllox};Sf1-cre* ovaries
212 compared to control ovaries at P14 and P18.

213



214

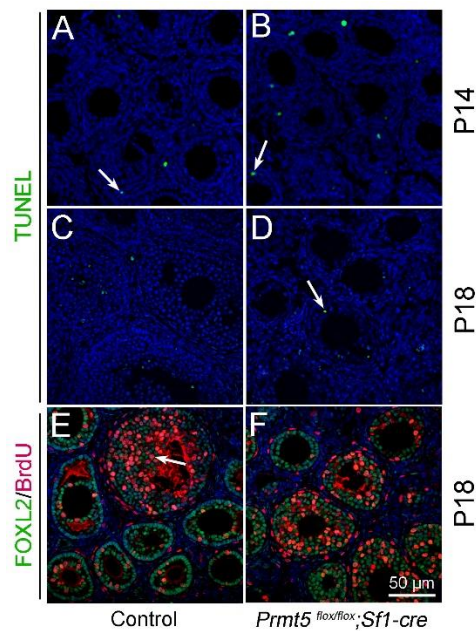
215 **Figure 3. The identity of granulosa cells in *Prmt5^{fllox/fllox};Sf1-cre* mice was changed.** The
216 expression of 3β-HSD, WT1, FOXL2, CYP11A1, and SF1 in ovaries of control and
217 *Prmt5^{fllox/fllox};Sf1-cre* mice at P18 was examined by immunofluorescence. In control ovaries,
218 3β-HSD (A), CYP11A1 (C), and SF1 (E) were expressed only in theca-interstitial cells (white
219 arrowheads). In the ovaries of *Prmt5^{fllox/fllox};Sf1-cre* mice, 3β-HSD (B), CYP11A1 (D), and SF1 (F)
220 were also detected in granulosa cells (white arrows). The arrows in H point to the disordered
221 follicle structure as shown by Laminin expression. DAPI (blue) was used to stain the nuclei.

222

223

224

225



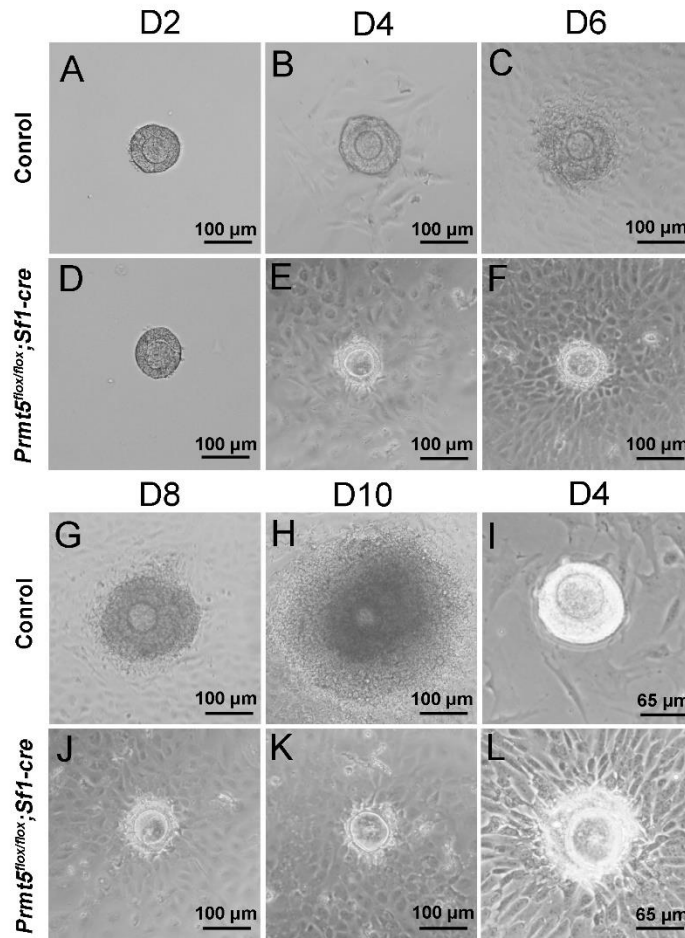
226

227 **Figure S4. The apoptosis and proliferation of granulosa cells was not changed in**
228 ***Prmt5^{flox/flox};Sf1-cre* mice at P14 and P18.** Apoptosis and cell proliferation were assessed by
229 TUNEL assay (A-D) and BrdU incorporation assay (E-F), respectively. The numbers of
230 TUNEL-positive cells and BrdU-positive cells were not different in *Prmt5^{flox/flox};Sf1-cre* ovaries
231 compared to control ovaries. DAPI (blue) was used to stain the nuclei.

232

233 To further confirm the above results, follicles were dissected from the ovaries of
234 2-week-old mice and cultured in vitro. As shown in Fig. 4, the morphology of follicles
235 from *Prmt5^{flox/flox};Sf1-cre* mice was comparable to that of control follicles at D2.
236 Proliferation of granulosa cells in control follicles was observed at D4, and the
237 follicles developed to the preovulatory stage with multiple layers of granulosa cells
238 after 9 days of culture (A-C, G-H). The granulosa cells were detached from oocytes in
239 *Prmt5^{flox/flox};Sf1-cre* follicles at D4 (E, and a magnified view in L), and no colonized
240 granulosa cells were observed after 9 days of culture (D-F, J-K). Most of the
241 granulosa cells were attached to the culture dishes just like the interstitial cells, and
242 denuded oocytes were observed after 3 days of culture (E-F, J-K, and a magnified

243 view in L).



244

245 **Figure 4. Aberrant development of in vitro-cultured *Prmt5^{flox/flox}; Sfl1-cre* follicles.** Follicles
246 with 2-3 layers of granulosa cells isolated from control and *Prmt5^{flox/flox}; Sfl1-cre* mice were
247 cultured in vitro. After 9 days of culture, control follicles grew significantly and developed to the
248 preovulatory stage (A-C, G-H). No obvious layers of granulosa cells were observed around
249 oocytes (D-F, J-K), and the granulosa cells extended away from the oocytes and adhered to the
250 dish (L). I and L are two magnified views of cultured follicles at day 4.

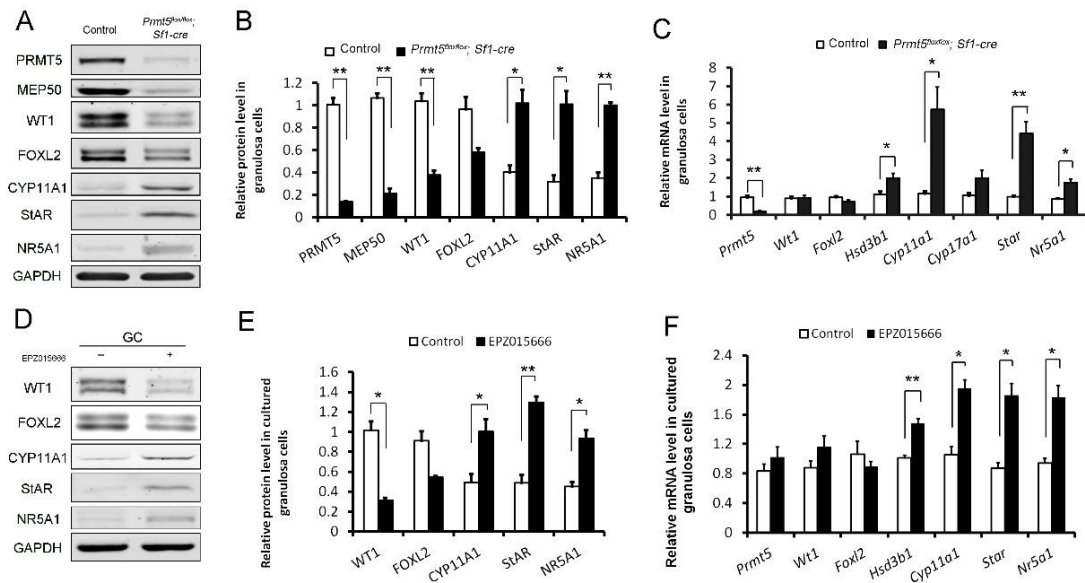
251

252 To further verify the differential expression of granulosa cell-specific and
253 steroidogenic genes in *Prmt5*-deficient granulosa cells, granulosa cells were isolated
254 at P18, and gene expression was analyzed by Western blot and real-time PCR
255 analyses. As shown in Fig. 5 (A, B), the protein levels of PRMT5 and its interacting
256 partner MEP50 were decreased dramatically in *Prmt5^{flox/flox}; Sfl1-cre* granulosa cells, as

257 expected. The protein level of WT1 was significantly reduced in *Prmt5*-deficient
258 granulosa cells. Surprisingly, the mRNA level of *Wt1* was not changed in
259 *Prmt5*-deficient granulosa cells (C). FOXL2 expression was also decreased, but the
260 difference was not significant. The expression of the steroidogenic genes CYP11A1,
261 StAR and NR5A1 was significantly increased in *Prmt5*-deficient granulosa cells,
262 consistent with the immunostaining results. Their mRNA levels were also
263 significantly increased (C). We also examined the functions of PRMT5 by treating
264 granulosa cells with the PRMT5-specific inhibitor EPZ015666. The protein level of
265 WT1 was significantly reduced after EPZ015666 treatment, whereas the mRNA level
266 was not changed. The expression of steroidogenic genes was significantly increased at
267 both the protein and mRNA levels after EPZ015666 treatment (Fig. 5D, E, F). These
268 results were consistent with those in *Prmt5*-deficient granulosa cells, indicating the
269 effect of PRMT5 on granulosa cells was dependent on its methyltransferase activity.
270 These results suggest that PRMT5 is required for maintenance of granulosa cell
271 identity and that inactivation of this gene causes granulosa cell-to-steroidogenic cell
272 transformation.

273

274



275

276 **Figure 5. Differentially expressed genes in *Prmt5*-deficient granulosa cells.** Western blot (A
 277 and B) and real-time PCR analyses (C) of the indicated genes in granulosa cells isolated from
 278 control or *Prmt5^{lox/lox};Sfl-cre* ovaries at P18. Western blot (D and E) and real-time PCR analyses
 279 (F) of the indicated genes in granulosa cells treated with DMSO or EPZ015666 (5 μ M) for 5 days.
 280 The protein expression in Western blot analysis was quantified and normalized to that of GAPDH
 281 (B and E). The data are presented as the mean \pm SEM. For B,E,F, n=3; For C, n=5. *, P < 0.05. **,
 282 P < 0.01.

283

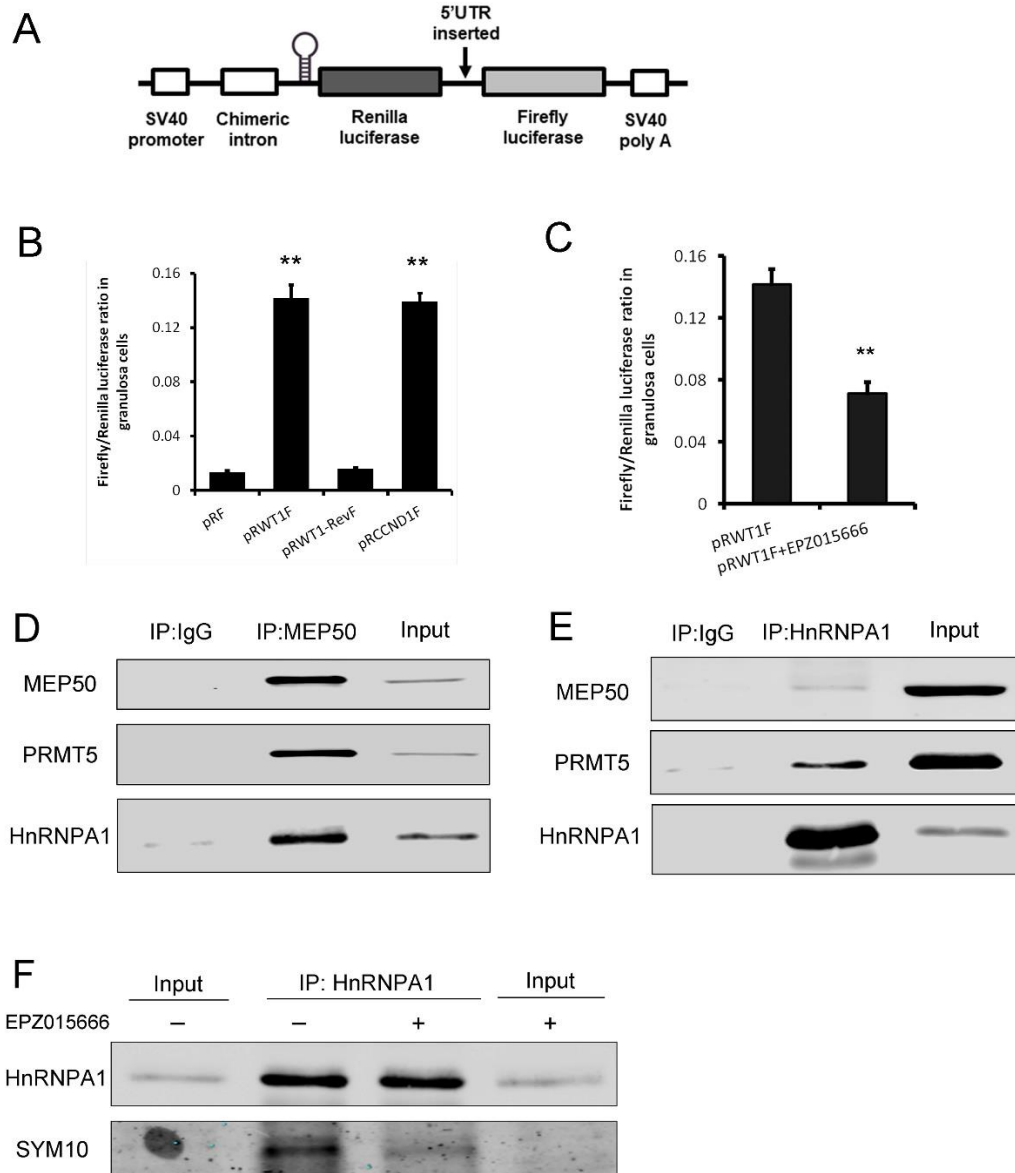
284 *The expression of WT1 was regulated by PRMT5 at the translational level*

285 PRMT5 has been reported to regulate the translation of several genes in an
 286 IRES-dependent manner^{17,18}. Internal ribosome entry sites (IRESs) are secondary
 287 structures in the 5'UTR that directly recruit the ribosome cap independently and
 288 initiate translation without cap binding and ribosome scanning¹⁹⁻²¹. *Wt1* 5'UTR is
 289 268bp, GC-rich (68%) and contains 7 CUG codons and 1 AUG codon. These features
 290 usually act as strong barriers for ribosome scanning and conventional translation
 291 initiation. Translation initiation in a number of these mRNAs is achieved via
 292 IRES-mediated mechanisms²¹. To test whether the *Wt1* 5'UTR contains an IRES
 293 element, we utilized a pRF dicistronic reporter construct in which upstream Renilla

294 luciferase is translated cap-dependently, whereas downstream firefly luciferase is not
295 translated unless a functional IRES is present. A stable hairpin structure upstream of
296 Renilla luciferase minimizes cap-dependent translation¹⁹ (Fig. 6A). *Wtl* 5'UTR was
297 inserted into the intercistronic region between Renilla and firefly luciferase (named
298 pRWT1F), and primary granulosa cells were transfected with pRF or pRWT1F. The
299 firefly/Renilla luciferase activity ratio was analyzed 48 hours later. As shown in Fig.
300 6B, the firefly/Renilla luciferase activity ratio was dramatically increased in
301 pRWT1F-transfected cells compared to pRF-transfected cells. In contrast, the
302 firefly/Renilla luciferase activity ratio was not increased when *Wtl* 5'UTR was
303 inserted in the reverse direction (pRWT1-RevF) (Fig. 6B). The luciferase activity was
304 dramatically increased with insertion of *Ccnd1* 5'UTR as a positive control, which
305 has been reported to contain an IRES element in the 5'UTR²². These results suggest
306 that *Wtl* 5'UTR probably contains an IRES element.

307 To verify that firefly luciferase protein was synthesized by translation of an
308 intact dicistronic transcript instead of a monocistronic mRNA generated by cryptic
309 splicing or promoter within the dicistronic gene²³, mRNA from pRF- or
310 pRWT1F-transfected cells was treated with DNase, reverse-transcribed, and then
311 amplified with primers binding to the 5' end of Renilla luciferase and 3' end of firefly
312 luciferase open reading frame spanning the whole transcript. Only one band was
313 detected in both cells with the expected molecular weight (Fig. S5A). Moreover,
314 qPCR analysis of firefly and Renilla luciferase mRNA levels also showed that the
315 firefly/Renilla luciferase mRNA ratio was not different between pRF- and

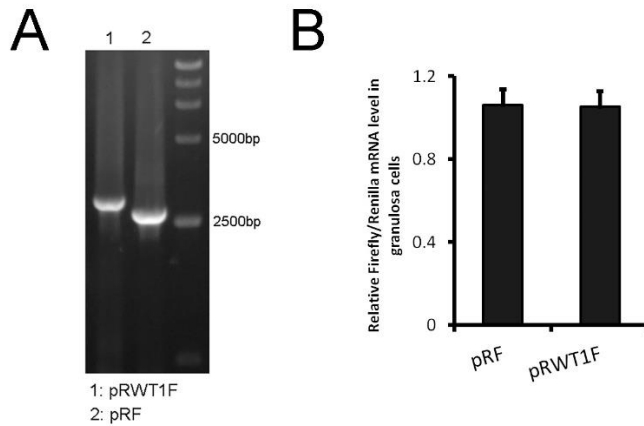
316 pRWT1F-transfected cells (Fig. S5B), further excluding the possibility that insertion
 317 of the *Wtl* 5'UTR into pRF generated a monocistronic firefly ORF.



318
 319 **Figure 6. PRMT5 regulated translation of *Wtl* mRNA by inducing IRES activity in the**
 320 **5'UTR.** A, Schematic representation of the dicistronic reporter construct. B, *Wtl* 5'UTR has IRES
 321 activity. Cultured primary granulosa cells were transfected with pRF, pRWT1F (pRF with the *Wtl*
 322 5'UTR inserted), pRWT1-RevF (pRF with the *Wtl* 5'UTR inserted in reverse orientation), or
 323 pRCCND1F (pRF with the *Ccnd1* 5'UTR inserted). The firefly and Renilla luciferase activities
 324 were measured 24 hours later, and the ratios of firefly luciferase activity to Renilla luciferase
 325 activity were calculated. C, Luciferase activity was decreased in primary granulosa cells treated
 326 with the PRMT5 inhibitor EPZ015666. Isolated granulosa cells were treated with DMSO or
 327 EPZ015666 for 4 days. The day granulosa cells were isolated was denoted as day 1. On day 4,
 328 granulosa cells were transfected with pRWT1F. Twenty-four hours later, the cells were harvested

329 for luciferase activity analysis. The ratios of firefly luciferase activity to Renilla luciferase activity
330 were calculated. In A-C, the data are presented as the mean \pm SEM, n=4. **, P < 0.01. D,
331 HnRNPA1 was pulled down with an antibody against the PRMT5-associated protein MEP50. E,
332 PRMT5 and MEP50 were pulled down by an HnRNPA1 antibody. F, The symmetric
333 dimethylation of HnRNPA1 was decreased after EPZ015666 treatment in primary granulosa cells.

334



335

336

337 **Figure S5. The increased luciferase activity of pRWT1F was not due to a monocistronic**
338 **firefly ORF generated by cryptic splicing or promoter within the dicistronic gene.** A, Primary
339 granulosa cells were transfected with pRF or pRWT1F plasmids. RNA was isolated,
340 DNase-treated, reverse-transcribed, and amplified using PCR primers that bind to the 5' end of
341 Renilla luciferase and the 3' end of the firefly luciferase sequence (A) or processed for real-time
342 PCR assays to analyze firefly and Renilla luciferase mRNA levels (B). The expression of firefly
343 luciferase mRNA was normalized to that of Renilla luciferase mRNA. The data are presented as
344 the mean \pm SEM, n=3.

345

346 To investigate the effect of PRMT5 on *Wtl* IRES activity, granulosa cells were
347 treated with EPZ015666 for 4 days, we found *Wtl* IRES activity was decreased
348 significantly by EPZ015666 (Fig. 6C). These results indicate that PRMT5 regulates
349 *Wtl* expression at the translational level through inducing its IRES activity in
350 granulosa cells.

351

352 *Wtl* IRES activity was regulated by PRMT5 through methylation of HnRNPA1

353 IRES-mediated translation depends on IRES *trans*-acting factors (ITAFs), which

354 function by associating with the IRES and either facilitate the assembly of initiation
355 complexes or alter the structure of the IRES^{23,24}. Heterogeneous nuclear
356 ribonucleoprotein A1 (HnRNPA1) is a well-studied RNA binding protein that plays
357 important roles in pre-mRNA and mRNA metabolism²⁵. HnRNPA1 is also an ITAF
358 that has been reported to regulate the IRES-dependent translation of many genes, such
359 as *Ccnd1*, *Apaf1*²⁶, *Myc*²⁴, *Fgf2*²⁷, and *Xiap*^{28,29}. HnRNPA1 can be methylated by
360 PRMT1²⁸ or PRMT5^{17,18}, which regulates the ITAF activity of HnRNPA1. To test
361 whether PRMT5 interacts with HnRNPA1 in granulosa cells, coimmunoprecipitation
362 experiments were conducted. We found that HnRNPA1 and PRMT5 were pulled
363 down by antibody against the PRMT5 main binding partner MEP50 (Fig. 6D).
364 Conversely, PRMT5 and MEP50 could be pulled down by the HnRNPA1 antibody
365 (Fig. 6E). We also found that the level of symmetric dimethylation of HnRNPA1 was
366 significantly reduced with EPZ015666 treatment in granulosa cells (Fig. 6F).

367 To test whether HnRNPA1 functions during PRMT5-mediated *Wt1* translation,
368 HnRNPA1 was knocked down in granulosa cells via siRNA transfection. Western blot
369 analysis results showed that HnRNPA1 protein levels were significantly decreased
370 with siRNA transfection (Fig. 7A). We found that WT1 protein level was increased
371 significantly in granulosa cells after knockdown of HnRNPA1. The decreased WT1
372 expression in EPZ015666-treated granulosa cells was partially reversed by
373 knockdown of HnRNPA1 (Fig. 7A). The luciferase activity of pRWT1F was increased
374 in granulosa cells with HnRNPA1 siRNA treatment and decreased in those with
375 EPZ015666 treatment. The decreased luciferase activity in EPZ015666-treated

376 granulosa cells was partially reversed by knockdown of HnRNPA1 (Fig. 7B). To
377 further confirm the effect of HnRNPA1 on *Wtl* IRES activity, HnRNPA1 was
378 overexpressed in granulosa cells, and we found that *Wtl* IRES activity was
379 significantly decreased (Fig. 7D). These results indicated that as an ITAF, the effect of
380 HnRNPA1 on *Wtl* IRES activity was repressive.

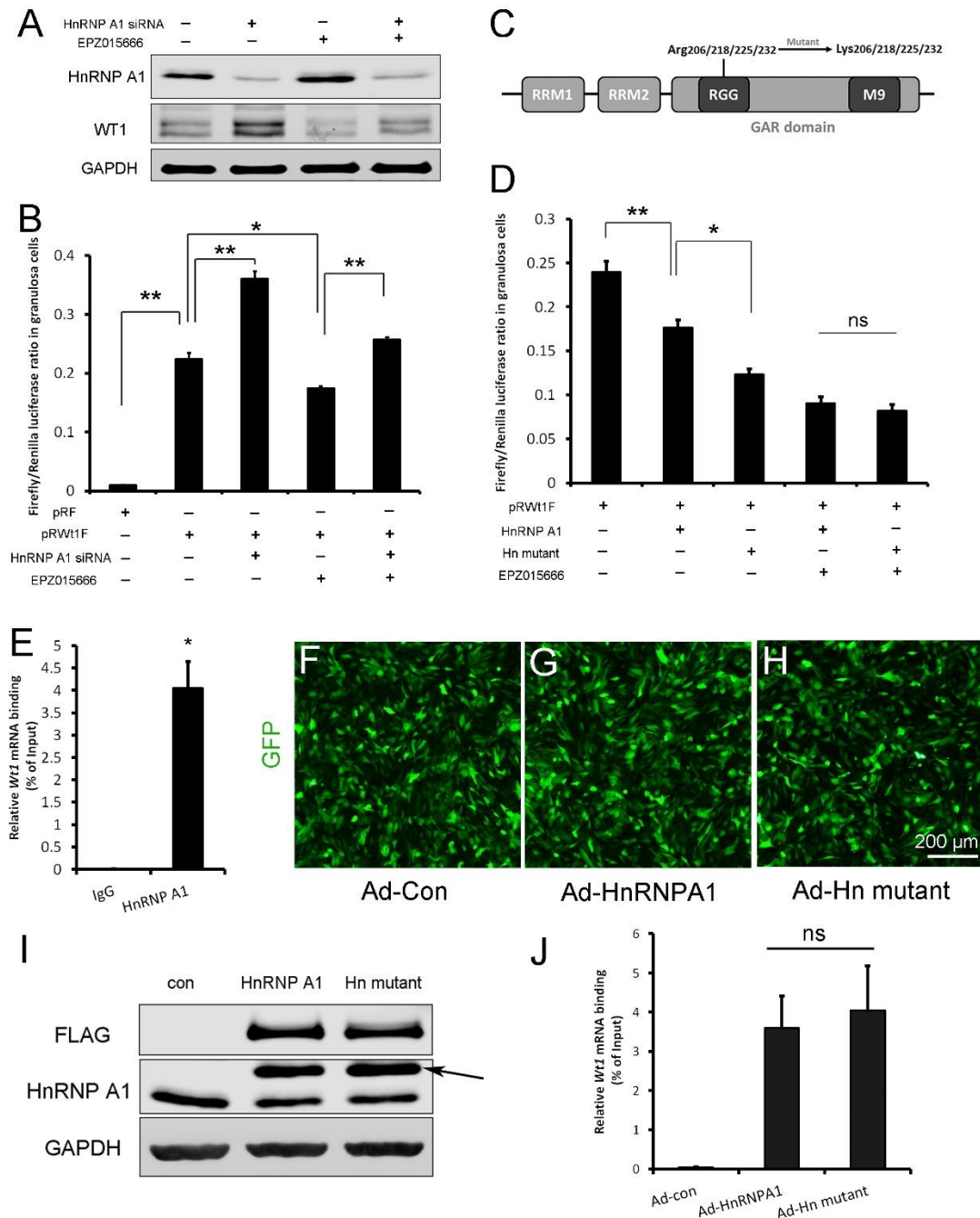
381 There are five arginine residues in the HnRNPA1 glycine/arginine-rich (GAR)
382 motif, which can be symmetrically or asymmetrically dimethylated by PRMT5¹⁷ or
383 PRMT1^{28,30}, respectively. R206, R218, R225 and R232 are required for HnRNPA1
384 ITAF activity^{17,28}. To determine the role of HnRNPA1 arginine methylation in *Wtl*
385 IRES activity, the four arginine residues were mutated to lysines (Fig. 7C), and
386 flag-tagged HnRNPA1 or mutant plasmids were cotransfected with pRWT1F into
387 granulosa cells. We found that *Wtl* IRES activity was further decreased in granulosa
388 cells overexpressing mutant HnRNPA1 compared to those overexpressing wild-type
389 HnRNPA1 (Fig. 7D). However, the difference in *Wtl* IRES activity between cells
390 overexpressing mutant HnRNPA1 and cells overexpressing wild-type HnRNPA1
391 disappeared when the granulosa cells were treated with EPZ015666 (Fig. 7D). These
392 results indicate that the repressive function of HnRNPA1 on *Wtl* IRES activity is
393 inhibited by PRMT5-mediated arginine symmetric dimethylation.

394

395

396

397



398

399 **Figure 7. *Wt1* IRES activity is regulated by PRMT5 via methylation of HnRNP A1.** A,
 400 Western blot analysis of HnRNP A1 and WT1 in granulosa cells after HnRNP A1 siRNA
 401 transfection or EPZ015666 treatment. B, Luciferase activity analysis of pRWT1F in granulosa
 402 cells after HnRNP A1 siRNA transfection or EPZ015666 treatment. Isolated granulosa cells were
 403 treated with DMSO or EPZ015666 for 4 days. The day granulosa cells isolated was denoted as
 404 day 1. On day 2, cells were transfected with control siRNA or siRNA to HnRNP A1. 48h later,
 405 pRF or pRWT1F were transfected. The luciferase activity of pRWT1F was calculated as the ratio
 406 of firefly luciferase activity to Renilla luciferase activity. C, Schematic diagram of HnRNP A1
 407 protein domains. HnRNP A1 contains two RRM (RNA recognition motifs). The
 408 glycine/arginine-rich (GAR) domain contains an RGG (Arg-Gly-Gly) box and a nuclear targeting
 409 sequence (M9). Four arginine residues within the RGG motif were mutated to lysine. D,

410 Luciferase activity analysis of pRWT1F in granulosa cells after EPZ015666 treatment or
411 overexpressing HnRNPA1 or arginine-mutated HnRNPA1. Isolated granulosa cells were treated
412 with DMSO or EPZ015666 for 4 days. On day 3, flag-tagged HnRNPA1 or mutant plasmids were
413 cotransfected with pRWT1F into granulosa cells. 48h later, cells were harvested for luciferase
414 activity analysis. E, RNA immunoprecipitation was conducted in granulosa cells using an
415 HnRNPA1 antibody, and the *Wtl* mRNA pulled down by HnRNPA1 was analyzed with real-time
416 PCR. F-H, Primary granulosa cells were cultured and infected with control, flag-tagged HnRNPA1,
417 or mutant HnRNPA1 (Ad-Hn mutant) adenoviruses. The expression of control and mutant
418 HnRNPA1 was examined by Western blot analysis (I). J, RNA immunoprecipitation was
419 conducted using a FLAG antibody, and *Wtl* mRNA pulled down by control or mutant HnRNPA1
420 protein was analyzed with real-time PCR. For B, D (n=4) and E, J (n=3), the data are presented as
421 the mean±SEM. *, P < 0.05. **, P < 0.01.

422

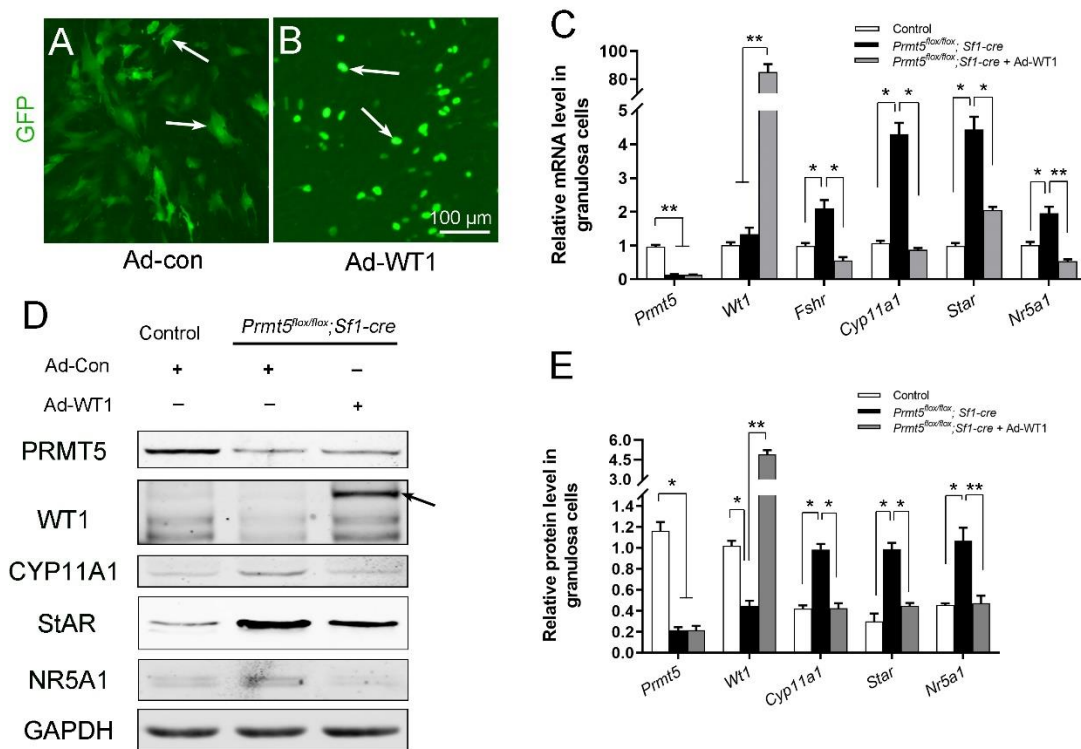
423 To test the interaction between HnRNPA1 and *Wtl* mRNA, RNA
424 immunoprecipitation was performed with an HnRNPA1 antibody in primary
425 granulosa cells. As shown in Fig. 7E, *Wtl* mRNA was pulled down by the HnRNPA1
426 antibody in granulosa cells. Next, granulosa cells were infected with flag-tagged
427 wild-type or arginine-mutant HnRNPA1 adenovirus (Fig. 7F-I) and RNA
428 immunoprecipitation was conducted with an FLAG antibody. The results showed that
429 mutation of arginines did not affect the interaction between HnRNPA1 and *Wtl*
430 mRNA (Fig. 7J).

431

432 *The upregulation of steroidogenic genes in Prmt5^{lox/lox};Sfl-cre granulosa cells was*
433 *repressed by Wtl overexpression.*

434 To test whether the upregulation of steroidogenic genes in *Prmt5*-deficient
435 granulosa cells is due to downregulation of WT1, granulosa cells from
436 *Prmt5^{lox/lox};Sfl-cre* mice were infected with control or GFP-tagged WT1-expressing
437 adenovirus (Fig. 8A, B). *Wtl* protein (Fig. 8D arrow, E) and mRNA (Fig. 8C) levels

438 were dramatically increased in *Prmt5*-deficient granulosa cells after *Wt1*
 439 overexpression. We found the expression of steroidogenic genes was significantly
 440 decreased in these cells. These results suggest that the aberrant differentiation of
 441 *Prmt5*-deficient granulosa cells can be rescued by WT1.
 442



443
 444
 445 **Figure 8. The upregulation of steroidogenic genes in *Prmt5^{flax/flax};Sf1-cre* granulosa cells was**
 446 **reversed by *Wt1* overexpression.** A, B, Granulosa cells isolated from control and
 447 *Prmt5^{flax/flax};Sf1-cre* mice were cultured and infected with control or GFP-fused *Wt1* adenovirus.
 448 The expression of steroidogenic genes was examined by RT-qPCR (C) and Western blot analysis
 449 (D). The protein expression in Western blot analysis was quantified and normalized to that of
 450 GAPDH (E). C,E, the data are presented as the mean \pm SEM (n=3). *, P < 0.05. **, P < 0.01.

451

452 Discussion

453 Protein arginine methylation is one of the most important epigenetic
 454 modifications and is involved in many cellular processes. It has been demonstrated

455 that PRMT5 is required for germ cell survival. In this study, we found that protein
456 arginine methylation plays important roles in granulosa cell development. The
457 development of ovarian follicles is a dynamic process. With follicle development, the
458 morphology and gene expression of granulosa cells are changed. When primordial
459 follicles are activated to grow, the flattened granulosa cells become more epithelial
460 through processes such as cuboidalization and polarization in primary follicles. The
461 granulosa cells in antral follicles express gonadotropin receptors. Before ovulation,
462 granulosa cells begin to express steroidogenic enzymes that are necessary for
463 progesterone and estradiol synthesis^{6,31}. WT1 is expressed at high levels in granulosa
464 cells of primordial, primary, and secondary follicles but decreases with follicle
465 development, suggesting it might be a repressor of ovarian differentiation genes in the
466 granulosa cells⁷. Our previous study demonstrated that the *Wtl* gene is required for
467 lineage specification and maintenance of granulosa cells^{8,9}. Inactivation of *Wtl* causes
468 the transformation of pregranulosa cells to steroidogenic cells. In this study, we found
469 *Prmt5*-deficient granulosa cells began to express steroidogenic genes in secondary
470 follicles and the upregulation of the steroidogenic genes in *Prmt5*-deficient granulosa
471 cells was reversed by *Wtl* overexpression, indicating that PRMT5 is required for
472 preventing the premature differentiation of granulosa cells via regulation of WT1
473 expression. Coordinated interaction between granulosa cells and oocytes is required
474 for successful follicle development and production of fertilizable oocytes. The
475 premature luteinized granulosa cells will lose their structural and nutritional support
476 for oocytes which will lead to follicle growth arrest or atresia at early stages of

477 folliculogenesis.

478 Our previous study demonstrated that WT1 represses *Sfl* expression by directly
479 binding to the *Sfl* promoter region and that inactivation of *Wtl* causes upregulation of
480 *Sfl*, which in turn activates the steroidogenic program⁸. In the present study, the
481 mRNA and protein levels of *Sfl* were significantly upregulated after WT1 loss;
482 therefore, the upregulation of steroidogenic genes in *Prmt5*-deficient granulosa cells
483 is due to the increased expression of *Sfl*.

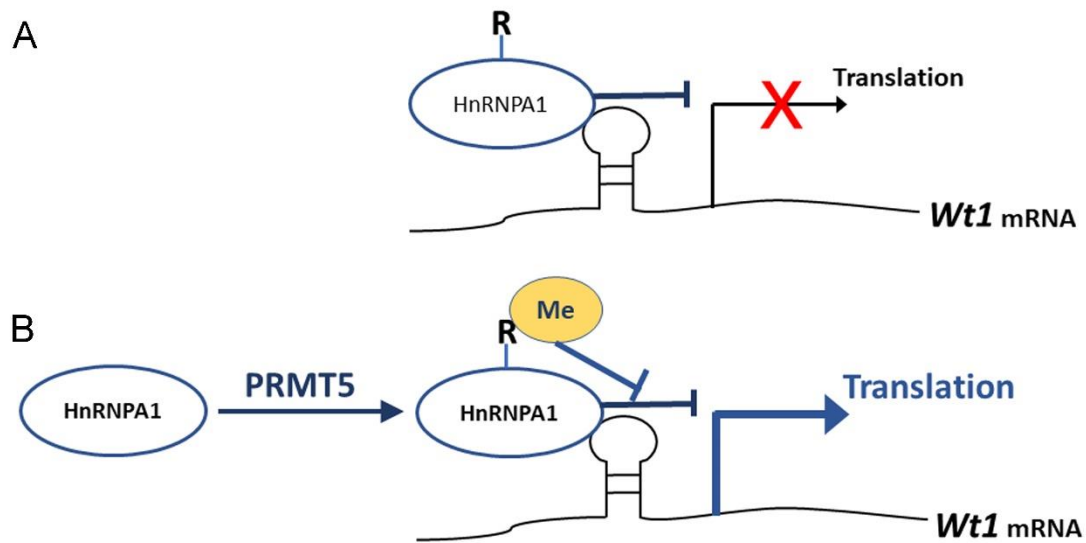
484 As an important nuclear transcription factor, the function of WT1 in granulosa
485 cell development has been investigated. However, the molecular mechanism that
486 regulates the expression of this gene is unknown. In this study, we found that the
487 expression of WT1 at the protein level was dramatically reduced in *Prmt5*-deficient
488 granulosa cells, whereas the mRNA level was not changed, indicating that PRMT5
489 regulates *Wtl* expression at the posttranscriptional level. In our mouse model, *Prmt5*
490 was inactivated in granulosa cells at the early embryonic stage. However, defects in
491 follicle development were not observed until 2 weeks after birth. Follicle development
492 was arrested. This outcome probably occurred because *Prmt5* is not expressed in
493 granulosa cells before the development of primary follicles (Fig. S1). During the early
494 stage, *Wtl* expression is also maintained in pre-granulosa cells, therefore, we
495 speculate there must be another factor(s) regulating *Wtl* expression before primary
496 follicle stage.

497 More than 100 mRNAs in mammals contain IRES elements in their 5'UTRs³²,
498 which are involved in various physiological processes, such as differentiation, cell

499 cycle progression, apoptosis and stress responses³³. The 5'UTR sequence of *Wtl*
500 mRNA is highly conserved, with more than 85% homology among the sequences of
501 29 mammalian species. Our study indicates that the *Wtl* 5'UTR has IRES activity.
502 HnRNPA1 belongs to the HnRNP family, which comprises at least 20 members
503 associated with RNA processing, splicing, transport and metabolism^{33,34}. As a main
504 ITAF, HnRNPA1 either activates the translation of *Fgf2*²⁷, *Srebp-1a*³⁵, and *Ccnd1*²² or
505 inhibits the translation of *Xiap*²⁹, *Apaf*²⁶, and *Bcl-xl*³⁶. The underlying mechanism by
506 which HnRNPA1 activates some IRESs but suppresses other IRESs is still unknown.
507 HnRNPA1 may compete with other ITAFs for binding or may modify IRES structure
508 and thus regulate IRES activity^{26,29}.

509 It has been reported that the expression of several genes is regulated by PRMT5
510 at the protein level^{17,37}. *Gao et al.* reported that PRMT5 regulates IRES-dependent
511 translation via methylation of HnRNPA1 in the 293T and MCF-7 cell lines. They
512 found that HnRNPA1 activates the IRES-dependent translation and that methylation
513 of HnRNPA1 facilitates the interaction of HnRNPA1 with IRES mRNA to promote
514 translation¹⁷. In the present study, we found that *Wtl* IRES activity was repressed by
515 HnRNPA1 (Fig. 9A) and that the repressive effect of HnRNPA1 was reversed by
516 PRMT5-mediated arginine methylation; thus, *Wtl* IRES-dependent translation was
517 promoted by PRMT5 (Fig. 9B).

518



519

520

521 **Figure 9. Schematic illustration of how PRMT5 regulates *Wt1* mRNA translation.** A, As an
522 ITAF, HnRNPA1 binds to *Wt1* mRNA and inhibits the IRES-dependent translation of *Wt1*. B,
523 PRMT5 catalyzes symmetric methylation of HnRNPA1, which suppresses the ITAF activity of
524 HnRNPA1 and promotes the translation of *Wt1* mRNA. R, arginine. Me, methylation.

525

526 The ITAF activity of HnRNPA1 can be regulated by posttranslational
527 modifications³³. Phosphorylation of HnRNPA1 on serine 199 by Akt inhibits
528 IRES-dependent translation of *c-myc* and *cyclin D1*^{22,24}. Symmetric dimethylation of
529 HnRNPA1 by PRMT5 enhances HnRNPA1 ITAF activity and promotes the
530 translation of target mRNAs¹⁷. Asymmetric dimethylation of HnRNPA1 by PRMT1
531 inhibits its ITAF activity²⁸. These results suggest that arginine methylation has
532 different effects on the ITAF activity of HnRNPA1 according to different IRESs and
533 cell contexts. Our study demonstrated that HnRNPA1 ITAF activity toward *Wt1*
534 mRNA was repressed by PRMT5-mediated arginine methylation. However, the
535 affinity between HnRNPA1 and *Wt1* mRNA was not affected after mutation of
536 arginine residues, consistent with the findings of a previous study²⁸. Therefore, the

537 inhibition of HnRNPA1 ITAF activity by PRMT5 does not occur through changes in
538 the binding of HnRNPA1 to *Wt1* mRNA. The underlying mechanism needs further
539 investigation.

540 Epigenetic modification is involved in numerous cellular processes. However,
541 the functions of epigenetic modification in granulosa cell development have not been
542 well studied. In this study, we demonstrated that *Prmt5* is required for maintenance of
543 granulosa cell identity in follicle development and that inactivation of *Prmt5* causes
544 premature luteinization of granulosa cells. Our study also demonstrates that PRMT5
545 regulates WT1 expression at the translational level by methylating HnRNPA1. This
546 study provides very important information for better understanding the regulation of
547 gonad somatic cell differentiation.

548

549 **Materials and Methods**

550 *Mice*

551 All animal experiments were carried out in accordance with the protocols
552 approved by the Institutional Animal Care and Use Committee at the Institute of
553 Zoology, Chinese Academy of Sciences (CAS). All mice were maintained on a
554 C57BL/6;129/SvEv mixed background. *Prmt5^{flox/flox}; Sfl-cre* female mice were
555 obtained by crossing *Prmt5^{flox/flox}* mice with *Prmt5^{+flox}; Sfl-cre* mice. *Prmt5^{flox/flox}* and
556 *Prmt5^{+flox}* female mice were used as controls.

557

558 *Plasmid and adenovirus*

559 The dicistronic construct pRF was a generous gift from Professor Anne Willis,
560 University of Cambridge. pRWT1F, pRCCND1F and pRWT1-RevF were constructed
561 by inserting the mouse *Wt1* 5'UTR, human *Ccnd1* 5'UTR or mouse *Wt1* 5'UTR in
562 reverse orientation into EcoRI and NcoI sites of the pRF vector. Mouse *Wt1* 5'UTR
563 and human *Ccnd1* 5'UTR sequence were amplified by PCR and the primers used
564 were: pRWT1F-F: CCGGAATTCTGTGTGAATGGAGCGGCCGAGCAT,
565 pRWT1F-R: CTAGCCATGGGATCGCGGCGAGGAGGCG; pRWT1-RevF-F:
566 CTAGCCATGGTGTGTGAATGGAGCGGCCGAGCAT, pRWT1-RevF-R:
567 CCGGAATTCGATCGCGGCGAGGAGGCG; pRCCND1F-F:
568 GCTGAATTCCACACGGACTACAGGGGAGTTTT, pRCCND1F-R:
569 CGGCCATGGGGCTGGGGCTCTTCCTGGGC. The primers amplifying the whole
570 transcript of pRF binding to the 5' end of renilla and 3' end of firefly ORF: pRF-F:
571 GCCACCATGACTTCGAAAGTTTATGA; pRF-R: TTACACGGCGATCTTTCCGC.
572 FLAG-tagged HnRNPA1 and mutant plasmids were generated by inserting the coding
573 sequence and a mutant sequence of mouse HnRNPA1, respectively, into NheI and
574 BamHI sites of the pDC316-mCMV-ZsGreen-C-FLAG vector. HnRNPA1-F:
575 CTAGCTAGCCACCATGTCTAAGTCCGAGTCTCCCAAGGA, HnRNPA1-R:
576 CGCGGATCCGAACCTCCTGCCACTGCCATAGCTA. Adenoviruses containing
577 WT1 coding sequence, HnRNPA1 or the mutant sequence were generated using the
578 Gateway Expression System (Invitrogen).

579

580 *Isolation of granulosa cells, transient transfection, infection and luciferase assay*

581 Granulosa cells were isolated from mice at 16-18 days old. After mechanical
582 dissection, ovaries were cut into several parts and incubated in PBS containing 1
583 mg/ml collagenase IV (Sigma) in a water bath with circular agitation (85 rpm) for 5
584 min at 37°C. Follicles were allowed to settle and washed in PBS. The supernatant
585 were discarded. A second enzyme digestion was performed in PBS containing 1
586 mg/ml collagenase IV, 1 mg/ml Hyaluronidase, 0.25% Trypsin, and 1mg/ml DNase I
587 (Applichem) for 15min. FBS was added to stop the digestion and cell suspension was
588 filtered through a 40- μ m filter. Cells were centrifuged, washed and then plated in
589 24-well plate in DMEM/F12 supplemented with 5% FBS. For EPZ015666 treatment,
590 granulosa cells were incubated in the medium with the addition of 5 μ M EPZ015666
591 (MedChemExpress) for 4-5 days. When cells were approximately 70% confluent,
592 granulosa cells were transfected with plasmids or infected with adenovirus according
593 to the experiments. At the end of culture, cells were lysed for RT-qPCR, Western blot
594 analysis, or luciferase activity analysis using a dual luciferase reporter assay system
595 (Promega).

596 Control siRNA or siRNA to HnRNPA1 was purchased from ThermoFisher
597 (S67643, S67644) and transfected into granulosa cells with Lipofectamine 3000
598 transfection reagent without P3000. 48 hours later, pRF or pRWT1F were transfected
599 and luciferase activities were measured the following day.

600

601 *In vitro ovarian follicle culture*

602 Follicles were dissected and cultured as previously described³⁸. Briefly, ovaries

603 of 14-day-old mice were dissected aseptically using the beveled edges of two syringe
604 needles. Follicles with 2–3 layers of granulosa cells, a centrally placed oocyte, an
605 intact basal membrane and attached theca cells were selected and cultured
606 individually in 20 μ l droplets of culture medium (α MEM supplemented with 5% FBS,
607 1% ITS and 100 mIU/ml recombinant FSH). The culture were maintained in 37°C
608 and 5% CO₂ in air. The medium was replaced every other day. The morphology of the
609 follicles was recorded daily under a microscope.

610

611 *Co-immunoprecipitation*

612 Granulosa cells isolated from mice at 16-18 days old were cultured in 10-cm
613 dishes and lysed with lysis buffer (50mM Tris·HCl (pH 7.5), 150 mM NaCl, 1mM
614 EDTA, 1% Nonidet P-40) supplemented with protease inhibitors cocktail (Roche) and
615 1mM PMSF. One milligram of protein were first pre-cleared with protein G agarose
616 beads (GE) for 1 hour at 4°C, then incubated with 1.5 μ g of IgG (mouse, Santa Cruz,
617 sc-2025; rabbit, Abmart, B30011S), HnRNPA1 antibody (Abcam, ab5832), or MEP50
618 antibody (Abcam, ab154190) for 4 hours at 4°C. Then protein A and G agarose beads
619 were added and incubated overnight. The immunoprecipitates were washed 4 times in
620 lysis buffer supplemented with cocktail and PMSF, resolved in loading buffer,
621 incubated for 5 min at 95°C, and then analyzed by Western blotting. The antibodies
622 used in Western blotting include: PRMT5 (Millipore, 07-405), SYM10 (Millipore,
623 07-412), HnRNPA1 (Abcam, ab5832), MEP50 (Abcam, ab154190).

624

625 *Western blot analysis*

626 Granulosa cells were washed with PBS, lysed with RIPA buffer (50 mM Tris–
627 HCl (pH 7.5), 150 mM NaCl, 1% NP-40, 0.1% SDS, 1% sodium deoxycholate, 5mM
628 EDTA) supplemented with protease inhibitors cocktail (Roche) and 1mM PMSF.
629 30µg total protein was separated by SDS/PAGE gels, transferred to nitrocellulose
630 membrane, probed with the primary antibodies. The images were captured with the
631 ODYSSEY Sa Infrared Imaging System (LI-COR Biosciences, Lincoln, NE, USA).
632 The antibodies used were: PRMT5 (Millipore, 07-405), MEP50 (Abcam, ab154190),
633 WT1 (Abcam, ab89901), FOXL2 (Abcam, ab5096), CYP11A1 (Proteintech,
634 13363-1-AP), StAR (Santa Cruz, sc-25806), SF1 (Proteintech, 18658-1-AP), FLAG
635 (Sigma, F1804).

636

637 *RNA immunoprecipitation*

638 Granulosa cells were isolated from mice at 16-18 days old and cultured in 10-cm
639 dishes. The cells were then lysed with RIP buffer (50 mM Tris-HCl pH7.5, 150 mM
640 NaCl, 5mM EDTA, 1% NP-40, 0.5% sodium deoxycholate) supplemented with
641 protease inhibitor cocktail and 200U/ml RNase inhibitor. 5% of the cell lysate
642 supernatants were used as the input and the remainings were incubated with 1.5 µg of
643 IgG (mouse, Santa Cruz, sc-2025), HnRNPA1 antibody (Abcam, ab5832), or FLAG
644 antibody (Sigma, F1804) for 4 hours at 4°C. Then protein A and G agarose beads were
645 added to immunoprecipitate the RNA/protein complex. The conjugated beads were
646 thoroughly washed with lysis buffer (50 mM Tris–HCl pH7.5, 500 mM NaCl, 5mM

647 EDTA, 1% NP-40, 0.5% sodium deoxycholate) supplemented with cocktail and
648 200U/ml RNase inhibitor. Bound RNA was extracted using a RNeasy Kit and
649 analyzed with RT-qPCR analysis.

650

651 *Real-time RT-PCR*

652 Total RNA was extracted using a RNeasy Kit (Aidlab, RN28) in accordance with
653 the manufacturer's instructions. One micrograms of total RNA was used to synthesize
654 first-strand cDNA (Abm, G592). cDNAs were diluted and used for the template for
655 real-time SYBR Green assay. *Gapdh* was used as an endogenous control. All gene
656 expression was quantified relative to *Gapdh* expression. The relative concentration of
657 the candidate gene expression was calculated using the formula $2^{-\Delta\Delta CT}$. Primers used
658 for the RT-PCR are listed in Table S1.

659

660 *Immunohistochemistry and immunofluorescence analysis*

661 Immunohistochemistry procedures were performed as described previously³⁹.
662 Stained sections were examined with a Nikon microscope, and images were captured
663 by a Nikon DS-Ri1 CCD camera. For immunofluorescence analysis, the 5- μ m
664 sections were incubated with 5% BSA in 0.3% Triton X-100 for 1 hours after
665 rehydration and antigen retrieval. The sections were then incubated with the primary
666 antibodies for 1.5 hours and the corresponding FITC-conjugated donkey anti-goat IgG
667 (1:150, Jackson ImmunoResearch) and CyTM3-conjugated donkey anti-rabbit IgG
668 (1:300, Jackson ImmunoResearch) for 1 hour at room temperature. The following

669 primary antibodies were used: WT1 (Abcam, ab89901), FOXL2 (Abcam, ab5096),
670 CYP11A1 (Proteintech, 13363-1-AP), SF1 (Proteintech, 18658-1-AP), 3 β -HSD
671 (Santa Cruz Biotechnology, sc-30820). After being washed three times in PBS, the
672 nuclei were stained with DAPI. The sections were examined with a confocal laser
673 scanning microscope (Carl Zeiss Inc., Thornwood, NY).

674

675 *Statistical analysis*

676 All experiments were repeated at least three times. For immunostaining, one
677 representative picture of similar results from three to five control or *Prmt5*-deficient
678 ovaries at each time point is presented. The quantitative results are presented as the
679 mean \pm SEM. Statistical analyses were conducted using GraphPad Prism version 9.0.0.
680 Unpaired two-tailed Student's t-tests were used for comparison between two groups.
681 For three or more groups, data were analyzed using one-way ANOVA. P-values <
682 0.05 were considered to indicate significance.

683

684 **Data availability**

685 Source data for Fig.5, 6, 7, 8 and Fig. S5 have been provided as Supplementary
686 file 1.

687

688 **Acknowledgments**

689 We thank Prof. Anne Willis (University of Cambridge) for her generous gift of
690 the dicistronic construct pRF. We thank Prof. Humphrey Hung-Chang Yao

691 (NIEHS/NIH) for the *Sfl-cre* mice. This work was supported by National key R&D
692 program of China (2018YFC1004200, 2018YFA0107700); Strategic Priority
693 Research Program of the Chinese Academy of Sciences (XDB19000000); The
694 National Science Fund for Distinguished Young Scholars (81525011); The National
695 Natural Science Foundation of China (31970785, 31601193, and 31671496).

696

697 **Author contributions**

698 F.G. and M.C. designed the experiments and wrote the manuscript. M.C. and
699 F.F.D. performed the experiments and analyzed the data. All authors discussed the
700 results and edited the manuscript. The authors declare that they have no conflict of
701 interest.

702

703 **References**

- 704 1 Monniaux, D. Driving folliculogenesis by the oocyte-somatic cell dialog: Lessons from genetic
705 models. *Theriogenology* **86**, 41-53, doi:10.1016/j.theriogenology.2016.04.017 (2016).
- 706 2 Richards, J. S. & Pangas, S. A. New insights into ovarian function. *Handb Exp Pharmacol*, 3-27,
707 doi:10.1007/978-3-642-02062-9_1 (2010).
- 708 3 Jagarlamudi, K. & Rajkovic, A. Oogenesis: transcriptional regulators and mouse models. *Mol*
709 *Cell Endocrinol* **356**, 31-39, doi:10.1016/j.mce.2011.07.049 (2012).
- 710 4 Liu, C. F., Liu, C. & Yao, H. H. Building pathways for ovary organogenesis in the mouse embryo.
711 *Curr Top Dev Biol* **90**, 263-290, doi:10.1016/S0070-2153(10)90007-0 (2010).
- 712 5 Oktem, O. & Urman, B. Understanding follicle growth in vivo. *Hum Reprod* **25**, 2944-2954,

- 713 doi:10.1093/humrep/deq275 (2010).
- 714 6 Smith, P., Wilhelm, D. & Rodgers, R. J. Development of mammalian ovary. *J Endocrinol* **221**,
- 715 R145-161, doi:10.1530/JOE-14-0062 (2014).
- 716 7 Hsu, S. Y. *et al.* Wilms' tumor protein WT1 as an ovarian transcription factor: decreases in
- 717 expression during follicle development and repression of inhibin-alpha gene promoter. *Mol*
- 718 *Endocrinol* **9**, 1356-1366, doi:10.1210/mend.9.10.8544844 (1995).
- 719 8 Chen, M. *et al.* Wt1 directs the lineage specification of sertoli and granulosa cells by
- 720 repressing Sf1 expression. *Development* **144**, 44-53, doi:10.1242/dev.144105 (2017).
- 721 9 Cen, C. *et al.* Inactivation of Wt1 causes pre-granulosa cell to steroidogenic cell
- 722 transformation and defect of ovary development. *Biol Reprod* **103**, 60-69,
- 723 doi:10.1093/biolre/iaaa042 (2020).
- 724 10 Karkhanis, V., Hu, Y. J., Baiocchi, R. A., Imbalzano, A. N. & Sif, S. Versatility of PRMT5-induced
- 725 methylation in growth control and development. *Trends Biochem Sci* **36**, 633-641,
- 726 doi:10.1016/j.tibs.2011.09.001 (2011).
- 727 11 Stopa, N., Krebs, J. E. & Shechter, D. The PRMT5 arginine methyltransferase: many roles in
- 728 development, cancer and beyond. *Cell Mol Life Sci* **72**, 2041-2059,
- 729 doi:10.1007/s00018-015-1847-9 (2015).
- 730 12 Di Lorenzo, A. & Bedford, M. T. Histone arginine methylation. *FEBS Lett* **585**, 2024-2031,
- 731 doi:10.1016/j.febslet.2010.11.010 (2011).
- 732 13 Li, Z. *et al.* The Sm protein methyltransferase PRMT5 is not required for primordial germ cell
- 733 specification in mice. *EMBO J* **34**, 748-758, doi:10.15252/embj.201489319 (2015).
- 734 14 Kim, S. *et al.* PRMT5 protects genomic integrity during global DNA demethylation in

- 735 primordial germ cells and preimplantation embryos. *Mol Cell* **56**, 564-579,
736 doi:10.1016/j.molcel.2014.10.003 (2014).
- 737 15 Wang, Y. *et al.* Protein arginine methyltransferase 5 (Prmt5) is required for germ cell survival
738 during mouse embryonic development. *Biol Reprod* **92**, 104,
739 doi:10.1095/biolreprod.114.127308 (2015).
- 740 16 Ikeda, Y. *et al.* Characterization of the mouse FTZ-F1 gene, which encodes a key regulator of
741 steroid hydroxylase gene expression. *Mol Endocrinol* **7**, 852-860,
742 doi:10.1210/mend.7.7.8413309 (1993).
- 743 17 Gao, G., Dhar, S. & Bedford, M. T. PRMT5 regulates IRES-dependent translation via
744 methylation of hnRNP A1. *Nucleic Acids Res* **45**, 4359-4369, doi:10.1093/nar/gkw1367 (2017).
- 745 18 Holmes, B. *et al.* The protein arginine methyltransferase PRMT5 confers therapeutic
746 resistance to mTOR inhibition in glioblastoma. *J Neurooncol* **145**, 11-22,
747 doi:10.1007/s11060-019-03274-0 (2019).
- 748 19 Coldwell, M. J., Mitchell, S. A., Stoneley, M., MacFarlane, M. & Willis, A. E. Initiation of Apaf-1
749 translation by internal ribosome entry. *Oncogene* **19**, 899-905, doi:10.1038/sj.onc.1203407
750 (2000).
- 751 20 Baird, S. D., Turcotte, M., Korneluk, R. G. & Holcik, M. Searching for IRES. *RNA* **12**, 1755-1785,
752 doi:10.1261/rna.157806 (2006).
- 753 21 Stoneley, M. & Willis, A. E. Cellular internal ribosome entry segments: structures, trans-acting
754 factors and regulation of gene expression. *Oncogene* **23**, 3200-3207,
755 doi:10.1038/sj.onc.1207551 (2004).
- 756 22 Shi, Y., Sharma, A., Wu, H., Lichtenstein, A. & Gera, J. Cyclin D1 and c-myc internal ribosome

- 757 entry site (IRES)-dependent translation is regulated by AKT activity and enhanced by
758 rapamycin through a p38 MAPK- and ERK-dependent pathway. *J Biol Chem* **280**, 10964-10973,
759 doi:10.1074/jbc.M407874200 (2005).
- 760 23 Kunze, M. M. *et al.* sST2 translation is regulated by FGF2 via an hnRNP A1-mediated
761 IRES-dependent mechanism. *Biochim Biophys Acta* **1859**, 848-859,
762 doi:10.1016/j.bbagrm.2016.05.005 (2016).
- 763 24 Jo, O. D. *et al.* Heterogeneous nuclear ribonucleoprotein A1 regulates cyclin D1 and c-myc
764 internal ribosome entry site function through Akt signaling. *J Biol Chem* **283**, 23274-23287,
765 doi:10.1074/jbc.M801185200 (2008).
- 766 25 Dreyfuss, G., Kim, V. N. & Kataoka, N. Messenger-RNA-binding proteins and the messages
767 they carry. *Nat Rev Mol Cell Biol* **3**, 195-205, doi:10.1038/nrm760 (2002).
- 768 26 Cammas, A. *et al.* Cytoplasmic relocalization of heterogeneous nuclear ribonucleoprotein A1
769 controls translation initiation of specific mRNAs. *Mol Biol Cell* **18**, 5048-5059,
770 doi:10.1091/mbc.e07-06-0603 (2007).
- 771 27 Bonnal, S. *et al.* Heterogeneous nuclear ribonucleoprotein A1 is a novel internal ribosome
772 entry site trans-acting factor that modulates alternative initiation of translation of the
773 fibroblast growth factor 2 mRNA. *J Biol Chem* **280**, 4144-4153, doi:10.1074/jbc.M411492200
774 (2005).
- 775 28 Wall, M. L. & Lewis, S. M. Methylarginines within the RGG-Motif Region of hnRNP A1 Affect
776 Its IRES Trans-Acting Factor Activity and Are Required for hnRNP A1 Stress Granule
777 Localization and Formation. *J Mol Biol* **429**, 295-307, doi:10.1016/j.jmb.2016.12.011 (2017).
- 778 29 Lewis, S. M. *et al.* Subcellular relocalization of a trans-acting factor regulates XIAP

- 779 IRES-dependent translation. *Mol Biol Cell* **18**, 1302-1311, doi:10.1091/mbc.e06-06-0515
780 (2007).
- 781 30 Rajpurohit, R., Lee, S. O., Park, J. O., Paik, W. K. & Kim, S. Enzymatic methylation of
782 recombinant heterogeneous nuclear RNP protein A1. Dual substrate specificity for
783 S-adenosylmethionine:histone-arginine N-methyltransferase. *J Biol Chem* **269**, 1075-1082
784 (1994).
- 785 31 Irving-Rodgers, H. F., Harland, M. L. & Rodgers, R. J. A novel basal lamina matrix of the
786 stratified epithelium of the ovarian follicle. *Matrix Biol* **23**, 207-217,
787 doi:10.1016/j.matbio.2004.05.008 (2004).
- 788 32 Jaud, M. *et al.* The PERK Branch of the Unfolded Protein Response Promotes DLL4 Expression
789 by Activating an Alternative Translation Mechanism. *Cancers (Basel)* **11**,
790 doi:10.3390/cancers11020142 (2019).
- 791 33 Godet, A. C. *et al.* IRES Trans-Acting Factors, Key Actors of the Stress Response. *Int J Mol Sci*
792 **20**, doi:10.3390/ijms20040924 (2019).
- 793 34 Roy, R., Huang, Y., Seckl, M. J. & Pardo, O. E. Emerging roles of hnRNPA1 in modulating
794 malignant transformation. *Wiley Interdiscip Rev RNA* **8**, doi:10.1002/wrna.1431 (2017).
- 795 35 Damiano, F. *et al.* hnRNP A1 mediates the activation of the IRES-dependent SREBP-1a mRNA
796 translation in response to endoplasmic reticulum stress. *Biochem J* **449**, 543-553,
797 doi:10.1042/BJ20120906 (2013).
- 798 36 Bevilacqua, E. *et al.* eIF2alpha phosphorylation tips the balance to apoptosis during osmotic
799 stress. *J Biol Chem* **285**, 17098-17111, doi:10.1074/jbc.M110.109439 (2010).
- 800 37 Nicholas, C. *et al.* PRMT5 is upregulated in malignant and metastatic melanoma and regulates

801 expression of MITF and p27(Kip1.). *PLoS One* **8**, e74710, doi:10.1371/journal.pone.0074710
 802 (2013).
 803 38 Gao, F. *et al.* Wt1 functions in ovarian follicle development by regulating granulosa cell
 804 differentiation. *Hum Mol Genet* **23**, 333-341, doi:10.1093/hmg/ddt423 (2014).
 805 39 Gao, F. *et al.* The Wilms tumor gene, Wt1, is required for Sox9 expression and maintenance of
 806 tubular architecture in the developing testis. *Proc Natl Acad Sci U S A* **103**, 11987-11992,
 807 doi:10.1073/pnas.0600994103 (2006).

808

809 **Table S1. Primers used for real-time PCR analysis.**

Gene Symbol	RT Forward Primer 5' to 3'	RT Reverse Primer 5' to 3'
<i>Prmt5</i>	TGGTGGCATAACTTTCGGACT	TCCAAGCCAGCGGTCAAT
<i>Wt1</i>	CAAGGACTGCGAGAGAAGGTTT	TGGTGTGGGTCTTCAGATGGT
<i>Hsd3b1</i>	CTCAGTTCTTAGGCTTCAGCAATTAC	CCAAAGGCAAGATATGATTTAGGA
<i>Cyp11a1</i>	CCAGTGTCCCCATGCTCAAC	TGCATGGTCCTTCCAGGTCT
<i>Cyp17a1</i>	GCCCAAGTCAAAGACACCTAAT	GTACCCAGGCGAAGAGAATAGA
<i>StAR</i>	CCGGAGCAGAGTGGTGTCA	CAGTGGATGAAGCACCATGC
<i>Sfl</i>	CCCAAGAGTTAGTGCTCCAGT	CTGGGCGTCTTTACGAGG
<i>Foxl2</i>	ACAACACCGGAGAAACCAGAC	CGTAGAACGGGAAGTGGCTA
<i>Fshr</i>	ATGTGTTCTCCAACCTACCCA	GCTGGCAAGTGTTAATGCCTG
<i>Gapdh</i>	GTCATTGAGAGCAATGCCAG	GTGTTGCTACCCCAATGTG
<i>Renilla</i>	CGTGGAACCATGTTGCCATCAA	ACGGGATTTACGAGGCCATGATA
<i>Firefly</i>	GGTTCCATCTGCCAGGTATCAGG	CGTCTTCGTCCAGTAAGCTATG

810